Electrochemical Studies of the Adsorption Behavior of Bovine Serum Albumin on Stainless Steel

Sasha Omanovic and Sharon G. Roscoe*

Department of Chemistry, Acadia University, Wolfville, Nova Scotia B0P 1X0, Canada

Received April 21, 1999. In Final Form: July 23, 1999

The adsorption behavior of bovine serum albumin (BSA) on high-purity austenitic low-carbon stainless steel and its effect on the state of the electrode surface have been studied over the temperature range 299−343 K under open-circuit-potential conditions, using electrochemical impedance spectroscopy (EIS). The impedance spectra were interpreted in terms of an equivalent electrical circuit (EEC) based on a possible physical model with the circuit elements representing the electrochemical properties of the investigated system. The adsorption of BSA onto the stainless steel surface resulted in an increased rate of metal dissolution, i.e., corrosion. The plateau values of corrosion rate were achieved after a "threshold" BSA concentration in the bulk solution at all the temperatures studied. The rate of the corrosion process was found to be controlled by both the surface diffusion and charge transfer process. Adsorption of BSA onto the stainless steel surface was described with a Langmuir adsorption isotherm. The thermodynamic data were calculated to give the corrosion activation energy, Gibbs free energy, enthalpy, and entropy of adsorption. The data suggested a very strong adsorption of BSA molecules, accompanied by a charge transfer mechanism involving chemisorption. An adsorption mechanism was proposed involving the interaction of the negatively charged carboxylate groups of the proteins with the stainless steel surface. The EIS technique was shown to be a valuable tool in studying the interfacial behavior of proteins at metal electrode surfaces.

Introduction

There has been considerable interest recently in the interfacial behavior of proteins, both in the food industry as a result of the problems associated with fouling[1,2] and with medical implant devices and biosensors[3−5] due to problems of bacterial growth and metal dissolution. For cases such as these, it is desirable to minimize protein adsorption. There are, however, other examples in which the adsorption of proteins on surfaces is desired, such as in the immobilization of enzymes and proteins for purification, separation, and biotechnology applications.[6] The interactions between proteins and surfaces, resulting in adsorption, can be determined from the properties of the proteins as well as other parameters such as the pH, concentration, and temperature of the system.[7]

The dairy industry has been confronted with fouling of metal surfaces since plate heat exchangers were introduced for pasteurizing and sterilizing milk.[1,2] For most of the heat exchangers used, cleaning of the equipment at least once per day is a common practice, which means that the process has to be temporarily stopped. Therefore, the overall costs of cleaning are very high. A large number of investigations to better understand the process of fouling have been reported,[8−10] but a real breakthrough in the complete control of fouling has not been reached. This is mainly due to the complexity of the dairy systems and a lack of understanding of the mechanism of fouling. However, it is generally agreed that the adsorption of proteins plays one of the most important roles in the overall process of fouling of the metallic surfaces.

Most metallic materials, used either in industry as materials of construction or in medicine as orthopedic implant devices, rely on the presence of passive films on their surface to develop good corrosion resistance. Conditions that adversely affect the integrity of these passive films and detract from its ability to control undesirable metal dissolution are the main concern in corrosion. With respect to the dairy industry and medicine, protein interactions with the passive film on the metal surface are therefore of considerable interest as they may have a bearing on film breakdown, metal ion release, and film repair processes.

Several studies have been conducted to evaluate the effect of proteins on the corrosion of some materials of interest to the dairy industry and medicine. It was generally established that proteins interact and alter the corrosion behavior in two ways: adsorption and chelation. Svare et al.[11] showed that bovine serum albumin (BSA) had little effect on the anodic dissolution of Cu or Ni. On the other hand Ni and Cd dissolved slowly in horse serum and appeared to be unaffected by the presence of oxygen.[12] They also found that Co dissolved rapidly in the horse serum forming Co complexes with proteins in the presence of oxygen. Clarke et al.,[13] using spectrophotometric methods, showed in their study of the effects of serum proteins (BSA and fibrinogen) on metallic corrosion that

* To whom correspondence should be addressed. Phone: (902) 585-1156 or (902) 585-1242. Fax: (902) 585-1114. e-mail: sharon.roscoe@acadiau.ca.

(1) Dejong, P. *Trends Food Sci. Technol.* **1997**, *8*, 401.
(2) Changani, S. D.; Belmarbeiny, M. T.; Fryer, P. J. *Exp. Therm. Fluid Sci.* **1997**, *14*, 392.
(3) Uniyal, S.; Brash, J. L.; Degterev, I. A. *Adv. Chem. Ser.* **1982**, *No. 199*, 272.
(4) Khan, M. A.; Williams, R. L.; Williams, D. F. *Biomaterials* **1996**, *17*, 2117.
(5) Kanagaraja, S.; Lundström, I.; Nygren, H.; Tengvall, P. *Biomaterials* **1996**, *17*, 2225.
(6) Fitzgerald, R. J.; Swaisgood, H. E. *Arch. Biochem. Biophys.* **1989**, *268*, 239.
(7) Kiss, E. *Colloids Surf. A: Physicochem. Eng. Aspects* **1993**, *76*, 135.
(8) Addesso, A.; Lund, D. B. *J. Food Process. Preserv.* **1997**, *21*, 319.
(9) Visser, H. *J. Dispersion Sci. Technol.* **1998**, *19*, 1127.
(10) Kim, J. C.; Lund, D. B. *J. Food Process Eng.* **1998**, *21*, 369.
(11) Svare, C. W.; Belton, G.; Korostoff, E. *J Biomed. Mater. Res.* **1970**, *4*, 457.
(12) Weinzierl, S. M.; Webb, W. *Br. J. Cancer* **1972**, *26*, 279.
(13) Clarke, G. C. F.; Williams, D. F. *J. Biomed. Mater. Res.* **1982**, *16*, 125.

10.1021/la990474f CCC: $18.00
Published on Web 09/03/1999

the proteins greatly enhanced the corrosion of the first row transition metals due to their ability to form complexes. Protein-catalyzed dissolution of these metals was also suggested. Williams et al.[14] found that 316L stainless steel and commercially pure Ti exhibited greater corrosion in the presence of serum proteins, contrary to the Ti-6Al-4V alloy. Hsu et al.[15] found that the pitting corrosion of 316L stainless steel surface in oxygenated solutions was higher for saline than for saline−serum solution. Woodman et al.[16] found that the predominant corrosion products from 316L stainless steel were organometallic complexes with serum proteins. Gel chromatography was used to fractionate the proteins with bound metal atoms. Metal binding was found to be dominant in two molar mass classes of proteins, viz., M_r 820 000 (α2-macroglobulin) and M_r 66 300 (albumin).

A number of studies have been made on the interaction of proteins with metal surfaces to determine the molecular conformation or orientation of the adsorbed molecules. Recent studies in our laboratory have been made on globular proteins such as β-lactoglobulin,[17−19] α-lactalbumin,[20] κ-casein,[21] ribonuclease,[18,19] lysozyme,[18,19] BSA,[20] insulin,[22] cytochrome *c*,[23] myoglobin,[23] and hemoglobin[23] at a platinum electrode. The surface charge density resulting from protein adsorption was found to be sensitive to the conformational behavior of the proteins. The carboxylate groups were determined to play a major role as the surface-active functional group of the proteins at anodic potentials and a mechanism has been proposed. However, it was also of interest to examine protein behavior at a typical industrial surface such as stainless steel. Thus, the present study was carried out to investigate the interfacial behavior of BSA at a high-purity austenitic low-carbon stainless steel electrode surface, using open circuit potential (OCP), potentiodynamic linear polarization (LP), and electrochemical impedance spectroscopy (EIS) techniques. The electrode/electrolyte interface and corresponding surface processes were modeled by applying an equivalent electrical circuit (EEC) approach. A temperature range of 299−343 K was used in the experiments.

Experimental Section

(i) Reagents and Solutions. The stock solutions of bovine serum albumin, BSA (Sigma Chemical Co., Product No. A-0281, fat free), were prepared by dissolving a proper amount of solid BSA in 0.05 M phosphate buffer solution pH 7.0, which was previously prepared using anhydrous monobasic potassium phosphate (KH_2PO_4, cell culture tested) and sodium hydroxide (prepared from standardized BDH Chemical Co. concentrate). Conductivity water (Nanopure, resistivity of 18.2 MΩ cm) was used in the preparation of all aqueous solutions. Working solutions of various BSA concentrations were prepared by mixing the required amount of the stock solution and phosphate buffer solution.

Table 1. Chemical Composition of Austenitic Stainless Steel (mass %)

Fe	Cr	Ni	Mn	Mo	C	Mg	Si	S	N
bulk	17	12			0.002	<0.0006	<0.0004	0.002	<0.0005

(ii) Electrochemical Equipment. A standard three-electrode cell was utilized. The counter electrode was a large-area platinum electrode (mesh) of high purity (99.99%, Johnson-Matthey), which was degreased by refluxing in acetone, sealed in soft glass, electrochemically cleaned by potential cycling in 0.5 M sulfuric acid, and stored in 98% sulfuric acid. The usage of a large-area electrode was particularly important for the impedance measurements since the impedance of a counter electrode must be negligible compared with the impedance of the working electrode. The reference electrode was a commercial saturated calomel electrode SCE (Accumet) separated from the cell electrolyte by a glass frit. All potentials in this paper are referred to the SCE. The working electrode was prepared from a stainless steel rod (obtained from AMES Laboratory, Iowa State University) that was sealed into a glass tube with epoxy resin (Torr Seal). The exposed geometrical area of the electrode was 0.054 cm^2, and a calculated roughness factor was 2.8. The value of the roughness factor was obtained from the EIS measurements made on the electrodes polished with 1500 grit paper and 1 μm diamond paste, for which a roughness factor was reported to be 1.6.[24] However, all the values in the paper are referred to the geometrical surface area. The chemical composition of the stainless steel used in this research is given in Table 1. Its composition corresponds to a high-purity austenitic low-carbon stainless steel.

An EG&G PAR model 273 potentiostat/galvanostat and a Solartron Frequency Response Analyzer model 1255, controlled by a 486 PC, were used in all measurements. Impedance measurements were made in a wide frequency range from 50 kHz to 10 mHz with the ac voltage amplitude of ±5 mV and 10 points per decade.

(iii) Experimental Methodology. Prior to each measurement, the working electrode was wet polished with emery paper down to 1500 grit, thoroughly rinsed with Nanopure water, degreased in acetone, and again rinsed with Nanopure water. This procedure ensured a reproducible surface state of the working electrode.

All measurements were carried out in an oxygen-free solution, which was achieved by continuous purging of the cell with nitrogen gas (Linde, commercial purity 99.7%), which was previously deoxygenated by passage through a copper furnace at 573 K. This bubbling also provided a well-mixed bulk solution. The protein solution was prepared in a separate container and allowed to equilibrate for at least 30 min in the constant-temperature bath, fitted with a Jubalo P temperature regulator, at the same temperature as the electrochemical cell. After the electrode was characterized for the electrochemical technique in the phosphate buffer, aliquots of protein were then added to the electrochemical cell and the electrochemical measurements were repeated with each aliquot.

Results and Discussion

Figure 1 shows the time dependence of the open circuit potential (OCP) of a stainless steel electrode immersed in a phosphate buffer solution at pH 7.0. This type of measurement gives information about the "natural" corrosion behavior of the system undisturbed by any external voltage or current source and, therefore, in the absence of induced corrosion effects. When the freshly polished electrode was immersed in the electrolyte, the potential fell sharply to a minimum value (Figure 1), followed by a gradual increase to a steady-state potential value of −0.641 mV, which was reached after ap-

(14) Williams, R. L.; Brown, S. A.; Merritt, K. *Biomaterials* **1988**, *9*, 181.
(15) Hsu, H. M.; Buchanan, R. A. *Prod. 10th Annual Meeting (University of Alabama: Soc. for Biomaterials)* **1984**, 124.
(16) Woodman, J. L.; Black, J.; Jimenez, S. A. *J. Biomed. Mater. Res.* **1984**, *18*, 99.
(17) Roscoe, S. G.; Fuller, K. L.; Robitaille, G. *J. Colloid Interface Sci.* **1993**, *160*, 245.
(18) Roscoe, S. G.; Fuller, K. L. *J. Colloid Interface Sci.* **1992**, *152*, 429.
(19) Roscoe, S. G. In *Modern Aspects of Electrochemistry*; Bockris, J. O'M., Conway, B. E., White, R. E., Eds.; Plenum Press: New York, 1996; Vol. 29, p 319.
(20) Rouhana, R.; Budge, S. M.; MacDonald, S. M.; Roscoe, S. G. *Food Res. Int.* **1997**, *30*, 303.
(21) Roscoe, S. G.; Fuller, K. L. *Food Res. Int.* **1993**, *26*, 343.
(22) MacDonald, S. M.; Roscoe, S. G. *J. Colloid Interface Sci.* **1996**, *184*, 449.
(23) Hanrahan, K. L.; MacDonald, S. M.; Roscoe, S. G. *Electrochim. Acta* **1996**, *41*, 2469.
(24) Bellanger, G.; Rameau, J. J. *J. Mater. Sci.* **1997**, *32*, 4355.

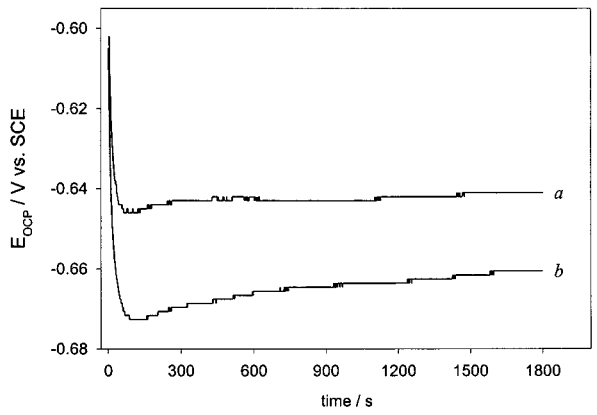

Figure 1. Time dependence of the open circuit potential of the stainless steel electrode in 0.05 M phosphate buffer solution pH 7.0 recorded at 313 K (a) without addition of BSA and (b) with addition of 0.0015 g L^{-1} of BSA.

Table 2. Redox Reactions and Corresponding Reversible Potentials at pH 7.0

$2Cr + 3H_2O \rightarrow Cr_2O_3 + 6H^+ + 6e^-$	-1.245 V[a] -1.309 V[b]	(1a)
$Fe + H_2O \rightarrow FeO + 2H^+ + 2e^-$	-0.729 V[a] -0.746 V[b]	(1b)
$2Fe + 3H_2O \rightarrow Fe_2O_3 + 6H^+ + 6e^-$	-0.710 V[a] -0.634 V[b]	(1c)
$2FeO + H_2O \rightarrow Fe_2O_3 + 2H^+ + 6e^-$	-0.673 V[a] -0.409 V[b]	(1d)
$Ni + H_2O \rightarrow NiO + 2H^+ + 2e^-$	-0.524 V[a] -0.516 V[b]	(1e)

[a] Dehydrated form of oxide. [b] Hydrated form of oxide.

proximately 30 min. From thermodynamic data,[25,26] the reversible potentials for the oxidation of the main constituents of the alloy at pH 7 were calculated, and the results are presented in Table 2. Transitions to higher oxidation states are not given, since their reversible potentials are much more positive than the observed OCP.

A comparison of the OCP value from Figure 1 (−0.641 V) to those listed in the table shows that the formation of Ni(II)-oxide/hydroxide (eq 1.e) could be excluded within the time domain of the experiment, and the remaining Cr and Fe transitions should be taken into account to describe the formation of a protective passive layer on the surface of the alloy. In this potential region, a passive film formed on a stainless steel surface consists of an inner Cr(III)-oxide/hydroxide layer and outer, very thin Fe(II)/(III)-oxide/hydroxide layer.[27−30] However, the Cr(III)-rich layer is mainly responsible for the high corrosion resistance of the alloy.[27,30] This layer is spontaneously formed on a freshly polished stainless steel surface immediately upon exposure to air and water and cannot be completely reduced, regardless of the applied cathodic potential.[27,28] While in contact with phosphate buffer, the Cr/Fe-rich layer thickened and stabilized with time, which resulted in a slight increase of the OCP (Figure 1).

Figure 1 also shows an OCP curve recorded after BSA was added to the phosphate buffer solution. Both curves

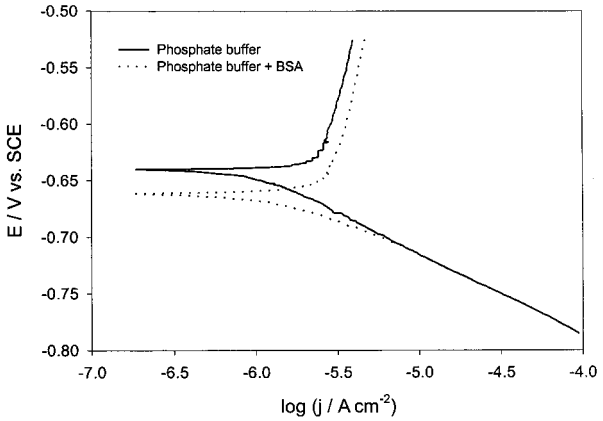

Figure 2. Tafel plots of the stainless steel electrode in 0.05 M phosphate buffer solution pH 7.0 without and with addition of 0.0015 g L^{-1} of BSA, recorded at 313 K. Scan rate was 0.5 mV s^{-1}.

have similar shapes, but the BSA curve is shifted toward more negative potentials, with a decrease of 20 mV in the final recorded OCP, compared to that measured in the pure phosphate solution. This indicates that BSA produced a change in the kinetics of the reactions occurring at the OCP on the stainless steel surface. Since the OCP measured in this experiment represents a mixed potential of metal dissolution and hydrogen evolution reactions, further investigations are required to determine which of the two processes is influenced by the addition of BSA.

The linear polarization curves (LP) for a stainless steel electrode were recorded without and with addition of BSA to the phosphate buffer solution after the electrode was held at the OCP for 30 min (Figure 2). Addition of BSA produced no change in the cathodic polarization branch corresponding to the hydrogen evolution reaction, as shown by the identical (overlaid) polarization curves. The value of the cathodic Tafel slope was calculated to be 70 mV $decade^{-1}$. However, a distinct change occurred in the anodic polarization branch that represents the response of the metal dissolution and subsequent passive film formation processes (eqs 1a−d). This means that BSA influenced only the kinetics of the anodic reactions. In addition, the shape of the anodic polarization curve indicates a participation of the diffusion processes in the reaction of metal dissolution, whereas the cathodic one resembles a purely activation (kinetic) controlled process.

The electrochemical impedance spectroscopy (EIS) technique was applied to further investigate the electrode/electrolyte interface and processes that occur on the surface in the presence of BSA molecules. To ensure complete characterization of the interface and surface processes, EIS measurements were made over seven frequency decades, from 50 kHz to 10 mHz, after the electrode was held at the OCP for 30 min. Figure 3 shows an example of an EIS spectrum recorded on a stainless steel electrode in a phosphate buffer solution. The presentation of the data in the form of a Nyquist impedance (complex) plot (Figure 3) clearly reveals the presence of two distinguishable time constants (τ_1 and τ_2), corresponding to the responses of two different processes. Thus, the EEC (Figure 4) comprised of the two time constants in parallel was used to model the experimental values. The fitting procedure showed that a better agreement between theoretical and experimental data was obtained if a frequency dependent constant phase element (CPE) was introduced instead of a pure capacitance (C). Generally, usage of a CPE is required due to a distribution of the relaxation times as a result of inhomogeneities present

(25) Stull, D. R.; Prophet, H. In *JANAF Thermochemical Tables*, 2nd ed.; NSRDS−NBS: Washington, DC, 1971.
(26) Hemmi, Y.; Ichikawa, N.; Saito, N.; Masuda, T. *J. Nucl. Sci. Technol.* **1994**, *31*, 1202.
(27) Drogowska, M.; Menard, H.; Brossard, L. *J. Appl. Electrochem.* **1996**, *26*, 217.
(28) Lorang, G.; Da Cunha Belo, M.; Simões, A. M. P.; Ferreira, M. G. S. *J. Electrochem. Soc.* **1994**, *141*, 3347.
(29) De Cristofaro, N.; Piantini, M.; Zacchetti, N. *Corros. Sci.* **1997**, *39*, 2181.
(30) Metikos-Hukovic, M.; Omanovic, S.; Babic, R.; Milosev, I. *Ber. Bunsen-Ges. Phys. Chem.* **1994**, *98*, 1243.

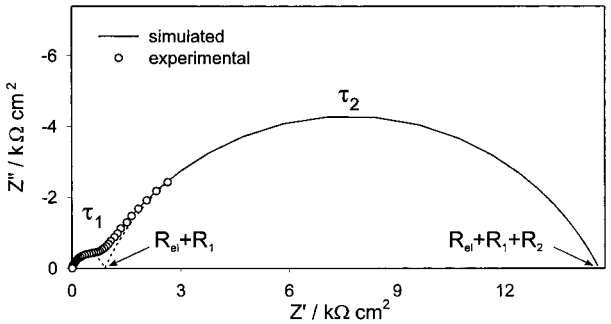

Figure 3. Nyquist plot of the stainless steel electrode in 0.05 M phosphate buffer solution pH 7.0, recorded at the OCP and 313 K.

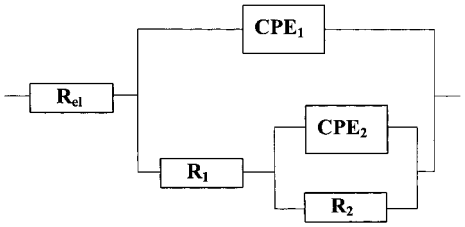

Figure 4. Equivalent electrical circuit used to model the EIS data recorded on the stainless steel electrode in 0.05 M phosphate buffer solution.

on the microscopic level under the oxide phase and at the oxide/electrolyte interface. This may result from contributions from static disorder such as porosity,[31] random mixture of conductor and insulator that can be described by the effective medium approximation at percolation,[32] or an interface that can be described by either a fractal geometry concept[33] or an RC transmission line concept.[34] The CPE can also include contribution from a dynamic disorder such as diffusion. The impedance of a constant-phase element is defined as[35]

$$Z_{\mathrm{CPE}} = [Q(j\omega)^n]^{-1} \qquad \text{with } -1 \le n \le 1 \qquad (2)$$

where Z (Ω cm^2) is the electrode impedance. The constant Q (Ω^{-1} s^n cm^{-2}) is a combination of properties related to both the surface and the electroactive species and is independent of frequency. The exponent n is related to a slope of the log Z against log f Bode plot, i.e., to the phase angle θ by the relation $n = 2\theta/\pi$ and $j = (-1)^{0.5}$. A pure capacitance yields $n = 1$, a pure resistance yields $n = 0$, a pure inductance yields $n = -1$, while $n = 0.5$ represents the Warburg impedance.

For all the experiments, the values of the CPE exponent n obtained by the fitting procedure were 0.90 ± 0.02 for the outer subcircuit (CPE_1-R_1) and 0.71 ± 0.06 for the inner one (CPE_2-R_2). From the values of the CPE and R obtained by modeling all the spectra, as well as from the spectrum in Figure 3, it was apparent that the outer subcircuit (CPE_1-R_1) had a much lower time constant than the inner one (CPE_2-R_2). Therefore, the outer subcircuit could be related to the fast charging/discharging processes detected at high frequencies, while the inner one then

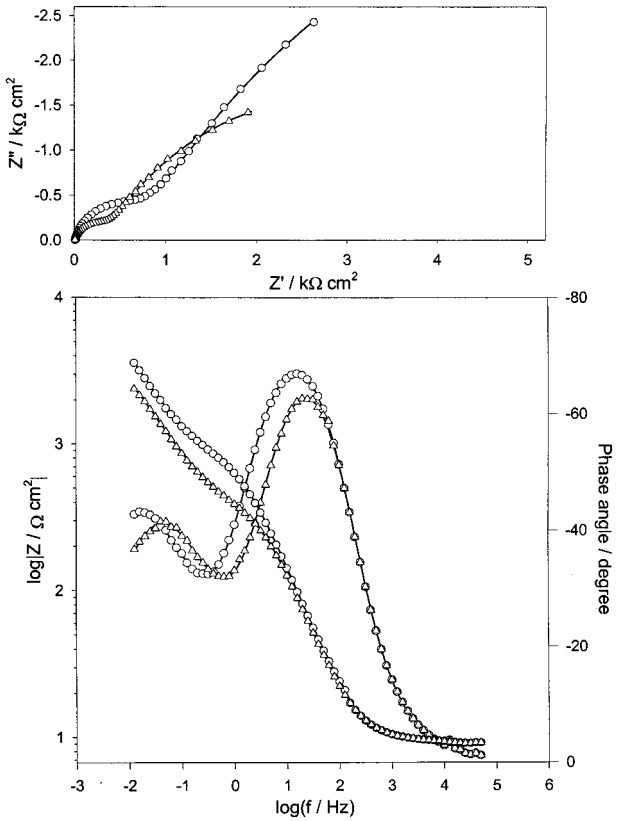

Figure 5. Nyquist and Bode plots of the stainless steel electrode in 0.05 M phosphate buffer solution pH 7.0, recorded at the OCP and 313 K (○) without and (△) with addition of 0.0015 g L^{-1} of BSA. Symbols are experimentally measured values and lines are simulated values.

represents the slower processes detected at low frequencies. Further, the value of the exponent n_2 was between the value corresponding to a pure charging process (capacitance) and pure diffusion process (Warburg impedance). Hence, the inner subcircuit (CPE_2-R_2) results from simultaneous occurrences of charge transfer and mass transport processes (diffusion); i.e., the process is said to be under mixed control. This is in agreement with the Tafel measurements (Figure 2), where the participation of diffusion processes was apparent in the anodic polarization branch. Jüttner et al.[36] interpreted the appearance of a similarly depressed semicircle ($0.5 < n < 1$) in the same manner. The change of a hydrodynamic regime in the cell did not influence the value of the CPE_2 and its exponent n_2, and therefore, the observed diffusion processes must have been in the solid phase, i.e., diffusion of the electroactive species occurred through the oxide phase. Similar conclusions were reported elsewhere.[27,28,37] Therefore, the outer subcircuit with the lower time constant τ_1 can be associated with the properties of the electrode/electrolyte interface, while the inner subcircuit, with the higher time constant τ_2, reflects the mass transport processes through the formed Cr/Fe-rich passive film.

Figure 5 shows the EIS spectra recorded on a stainless steel electrode immersed in a pure phosphate buffer solution (circles) and in a phosphate buffer solution containing BSA (triangles). Addition of BSA produced a significant decrease in the polarization resistance, R_p,

(31) Kramer, M.; Tomkiewicz, M. *J. Electrochem. Soc.* **1984**, *131*, 1283.
(32) Tomkiewicz, M.; Aurian-Blajeni, B. *J. Electrochem. Soc.* **1988**, *135*, 2743.
(33) Lin, H. S. *Phys. Rev. Lett.* **1985**, *55*, 529.
(34) Omanovic, S.; Metikos-Hukovic, M. *Thin Solid Films* **1995**, *266*, 31.
(35) Boukamp, B. A. In *Equivalent Circuit Users Manual*, Report CT88/265/128, University of Twente, Department of Chemical Technology, The Netherlands, 1989.
(36) Jüttner, K.; Lorenz, W. J.; Kending, M. W.; Mansfeld, F. *J. Electrochem. Soc.* **1988**, *135*, 332.
(37) Drogowska, M.; Ménard, H.; Lasia, A.; Brossard, L. *J. Appl. Electrochem.* **1996**, *26*, 1169.

Table 3. Results of the Fitting Procedure for the EIS Spectra Presented on Figure 5. R_{el} = 8.6 Ω cm²

EEC element	$c_{(BSA)}$ = 0 g L^{-1}	$c_{(BSA)}$ = 0.0015 g L^{-1}
$Q_1 \times 10^6/\Omega^{-1}$ s^n cm^{-2}	177.3	184.6
n_1	0.88	0.89
R_1/kΩ cm^2	0.87	0.41
$Q_2 \times 10^3/\Omega^{-1}$ s^n cm^{-2}	1.6	2.0
n_2	0.70	0.70
R_2/kΩcm^2	13.7	5.1
R_p/kΩcm^2	14.57	5.51

which is defined as an intersection of an extrapolated EIS curve in a Nyquist plot with the real axis[34] (Figure 3)

$$R_p = \lim_{\omega \to 0}[(Z_f)_{real}] \quad (3)$$

and therefore, the polarization resistance R_p is defined as the sum of the two resistors, $R_1 + R_2$. A nonlinear least-squares fit analysis (NLLS)[35] was employed in a modeling procedure, using the EEC presented in Figure 4. The impedance transfer function for this circuit could be written as

$$Z = R_{el} + \frac{R_1 + Z_W}{1 + Q_1(j\omega)^{n_1}(R_1 + Z_W)} \quad (4a)$$

where Z_W represents the impedance transfer function for the second time constant (CPE_2-R_2):

$$Z_W = \frac{R_2}{1 + Q_2(j\omega)^{n_2}R_2} \quad (4b)$$

A very good agreement between the experimental (symbols) and simulated (lines) values was obtained for all the measurements ($\chi^2 \approx (1-7) \times 10^{-5}$). The results for the representative spectra from Figure 5 are presented in Table 3.

To understand better the influence of BSA on the behavior of the stainless steel electrode surface, the dependence of the polarization resistance R_p was plotted versus the BSA concentration c_{BSA} for the whole range of temperatures investigated (Figure 6a−e). Figure 6f represents the normalized BSA quasi-polarization resistance curves $|\Delta R_{p,BSA}|$, obtained after subtracting the R_p value obtained in a BSA-free solution. Figure 6 directly illustrates the effect of the BSA on the stainless steel surface. A comparison of the curves presented in Figure 6 with those obtained on stainless steel (nonelectrochemical techniques)[38,39] and Pt electrodes (cyclic voltammetry)[20] show quite similar trends in behavior. The curves are similarly shaped but inversely proportional, which is expected if the reciprocal dependence between the polarization resistance and the charge or the surface concentration ($R_p \propto Q^{-1}$or Γ^{-1}) is taken into account. A plateau level was reached at each temperature after a concentration of approximately 5×10^{-4} g L^{-1} of BSA was acquired in the bulk solution (Figure 6).

When a stainless steel electrode is immersed in an electrolyte solution, it spontaneously starts to passivate by forming and/or improving the protective Cr/Fe-rich oxide film on its surface. This significantly inhibits further dissolution of the alloy and, thus, enhances its corrosion stability. Figure 6 shows that the addition of BSA to the phosphate buffer solution produced a decrease in polarization resistance, the value of which represents a direct measure of the metal dissolution rate, i.e., corrosion rate.[40] Therefore, the observed decrease of the polarization resistance values was a result of the increased dissolution rate of chromium and iron, most likely from the Cr/Fe passive oxide films. Investigations by Hansen et al.[38] of BSA adsorption on stainless steel 304L powder using nonelectrochemical methods showed that BSA produced significant amounts of Cr and Fe which were detected in solution. Clarke et al.,[13] using spectrophotometric methods, found that the proteins greatly enhanced the corrosion of the first row transition metals due to their ability to form complexes. Complexing of metal ions by proteins may reduce the activation energy or increase the chemical free-energy change associated with metal dissolution and enhance the corrosion rate of metals. Chelation of passive film-forming elements may disturb the local chemical equilibria, causing film dissolution and exposure of the underlying metal surface. Protein-catalyzed dissolution of these metals was also suggested. Merritt et al.[41] determined that almost all of the dissolved metal from a stainless steel 316L powder was bound to the albumin fraction of whole blood, with chromium and nickel representing the highest concentration of measured metals. Woodman et al.[42] found that serum albumin bound chromium, cobalt, and nickel from stainless steel 316L in the form of a corrosion product. The predominant form of the corrosion product of these metals was a metal−ligand complex, with the hydroxides of these metals complexing directly with albumin. Hansen et al.[38] concluded that the higher amount of dissolved Fe compared to Cr (ca. 10:1) was due to the higher concentration of Fe in the alloy. However, we would add that the higher concentration of dissolved Fe is, in addition, due to the fact that the Fe

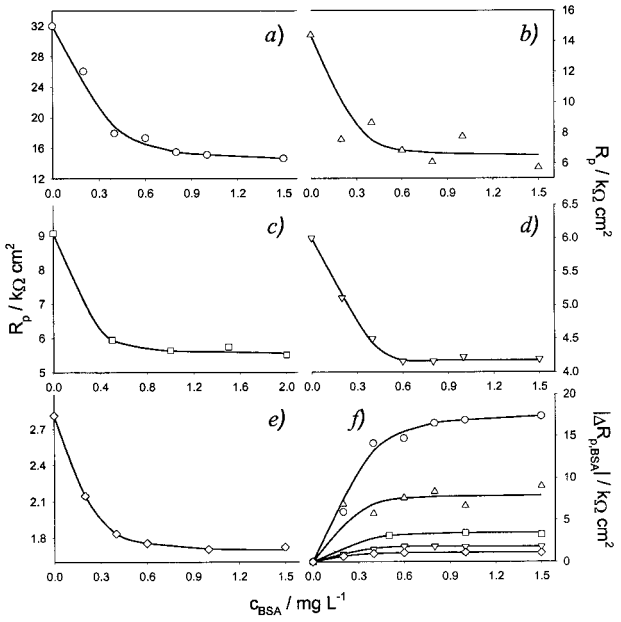

Figure 6. Dependence of the polarization resistance of the stainless steel electrode in 0.05 M phosphate buffer solution pH 7.0 containing different concentration of BSA. EIS measurements were made at the OCP at various temperatures: (a, ○), 299, (b, △) 313, (c, □) 323, (d, ▽) 333 and (e, ◇) 343 K.

(38) Hansen, D. C.; Luther, G. W., III; Waite, J. H. *J. Colloid Interface Sci.* **1994**, *168*, 206.

(39) Fukuzaki, S.; Urano, H.; Nagata, K. *J. Ferment. Bioeng.* **1995**, *80*, 6.

(40) ASTM G102: Standard Practice for Calculation of Corrosoin Rates and Related Information from Electrochemical Measurements, Annual Book of ASTM Standards, Section 3, Vol. 03.02, 1996; p 401.

(41) Merritt, K.; Brown, S. A.; Sharkey, N. A. *J. Biomed. Mater. Res.* **1984**, *18*, 1005.

(42) Woodman, J. L.; Black, J.; Jimenez, S. *Biomaterials* **1988**, *9*, 181.

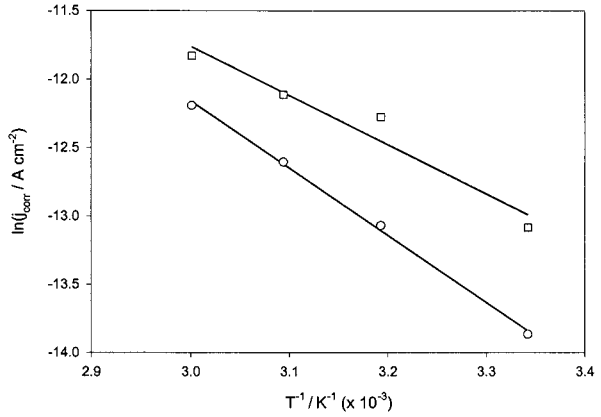

Figure 7. Arrhenius plots of the stainless steel electrode in 0.05 M phosphate buffer solution pH 7.0, (○) without and (□) with addition of BSA, obtained from EIS measurements at the OCP.

oxide layer forms on top of the preexisting Cr oxide layer and, therefore, dissolves more easily. Also, the Fe oxide layer is known to be much less compactly bound to the metallic surface than the Cr oxide.

The dependence of the rate of a metal dissolution process on temperature has been described using the Arrhenius equation:[43,44]

$$j_{\mathrm{corr}} = Ae^{-E_a/RT} \tag{5}$$

where j_{corr} (A cm^{-2}) is the corrosion current, E_a (J mol^{-1}) is the activation energy of corrosion, and A is a pre-exponential factor. The corrosion current can be calculated from the polarization resistance values using the well-known Stern−Geary equation:[40]

$$j_{\mathrm{corr}} = \frac{b_a b_c}{2.303(b_a + b_c)} \frac{1}{R_p} \tag{6}$$

where b_a and b_c (V decade^{-1}) are the anodic and cathodic Tafel slopes, respectively. However, since the anodic reaction in our case is under mixed control, b_a values could not be determined precisely. Therefore, the corrosion current could be approximated using just the cathodic Tafel slope:[40]

$$j_{\mathrm{corr}} = \frac{b_c}{2.303R_p} \tag{7}$$

Figure 7 shows the Arrhenius plots for the stainless steel electrode immersed in the phosphate buffer solution without and with addition of BSA. The j_{corr} values in the BSA-containing solution were calculated using polarization resistance values from the plateau regions (Figure 6). The activation energies, calculated from the slopes of the lines, were 40.9 kJ mol^{-1} for the BSA-free solution and 29.9 kJ mol^{-1} for the BSA-containing solution. Hence, the addition of BSA to the phosphate buffer solution caused a decrease in the corrosion activation energy of 11 kJ mol^{-1}. Such a significant decrease in the activation energy indicates that the adsorption of BSA molecules to the stainless steel surface occurred by a charge-transfer mechanism involving chemisorption.[45,46] Research in our laboratory[17−23] and elsewhere[47] has suggested that the adsorption of the proteins at the platinum and gold electrode surface under anodic conditions results from the interaction of the carboxylate functional groups of the acidic amino acid residues. These conclusions were based on kinetic measurements of the electron-transfer reaction mechanisms of amino acids.[48−51] Thus, in an analogous manner, the process occurring on the stainless steel surface at the OCP after addition of BSA could be described by the equation[17]

$$\mathrm{P} + n\mathrm{M} \rightarrow \mathrm{P(M)}_{n,\mathrm{ads}} + n\mathrm{e} \tag{8}$$

where P represents the protein adsorption on the metal (M) surface with n representing the number of sites for carboxylate interaction with the metal surface, accompanied by the transfer of a total of n electrons. An isoelectric point for BSA is 4.5,[14] and therefore it carries a negative charge at pH 7.0. The pH zero point of charge ($\mathrm{pH_{zpc}}$) for Fe-oxide/hydroxide, which is the outer oxide layer on a stainless steel surface, is 8.5.[38] Hence, at pH 7.0 the stainless steel surface at the OCP (Figure 1) has a net positive charge.[38] This will facilitate the involvement of negatively charged carboxylate groups of the proteins as anchoring sites in the contact region between the proteins and the stainless steel surface. Williams et al.[52] also noticed that the amount of BSA adsorbed was higher on metal surfaces with greater positive charge than on metals with negative charge. Similar conclusions of protein interaction with surfaces through the carboxylate groups are reported in the literature.[17−23,38,39,47−51,53]According to the literature,[38,39] adsorption of BSA onto the stainless steel surface has been described by the Langmuir isotherm

$$\Gamma = \frac{B_{\mathrm{ads}}\Gamma_{\mathrm{max}}c}{1 + B_{\mathrm{ads}}c} \tag{9}$$

in which c (mol cm^{-3}) is the equilibrium concentration of the adsorbate in the bulk solution, Γ (mol cm^{-2}) is the amount of protein adsorbed, i.e., surface concentration, Γ_{max} (mol cm^{-2}) is the maximum value of Γ, and the parameter B_{ads} (cm^3 mol^{-1}) reflects the affinity of the adsorbate molecules toward adsorption sites. Equation 9 can be rearranged to give:

$$\frac{c}{\Gamma} = \frac{1}{B_{\mathrm{ads}}\Gamma_{\mathrm{max}}} + \frac{c}{\Gamma_{\mathrm{max}}} \tag{10}$$

A plot of c/Γ versus concentration c should yield a straight line with parameters Γ_{max} and B_{ads} derived from the slope and intercept, respectively.

Figure 6 shows that the polarization resistance, i.e., corrosion current, depends on the BSA concentration. Therefore, the magnitude of the corrosion current, after being corrected for the current recorded in the BSA-free solution ($j_{\mathrm{corr,c}} = j_{\mathrm{corr,i}} - j_{\mathrm{corr,o}}$), can be correlated to the

(43) Metikos-Hukovic, M.; Babic, R.; Grubac, Z.; Brinic, S. *J. Appl. Electrochem.* **1996**, *26*, 443.
(44) Nagies, F.; Heusler, K. E. *Electrochim. Acta* **1998**, *43*, 41.
(45) Abdel Rahim, M. A.; Hassan, Hanaa B.; Khalil, M. *W. Materialwiss. Werkstofftech.* **1997**, *28*, 198.
(46) Stupnisek-Lisac, E.; Metikos-Hukovic, M.; Lencic, D.; Vorkapic-Furac, J.; Berkovic, K. *Corrosion* **1992**, *48*, 924.
(47) Liedberg, B.; Invarsson, B.; Hegg, P. O.; Lundström, I. *J. Colloid Interface Sci.* **1986**, *114*, 386.
(48) Marangoni, D. G.; Smith, R. S.; Roscoe, S. G. *Can. J. Chem.* **1989**, *67*, 921.
(49) Marangoni, D. G.; Wylie, I. G. N.; Roscoe, S. G. *Bioelectrochem. Bioenerg.* **1991**, *25*, 269.
(50) Wylie, I. G. N.; Roscoe, S. G. *Bioelectrochem. Bioenerg.* **1992**, *28*, 367.
(51) MacDonald, S. M.; Roscoe, S. G. *Electrochim. Acta* **1997**, *42*, 1189.
(52) Williams, R. L.; Williams, D. F. *Biomaterials* **1988**, *9*, 206.
(53) Fukuzaki, S.; Urano, H.; Nagata, K. *J. Ferment. Bioeng.* **1996**, *81*, 163.

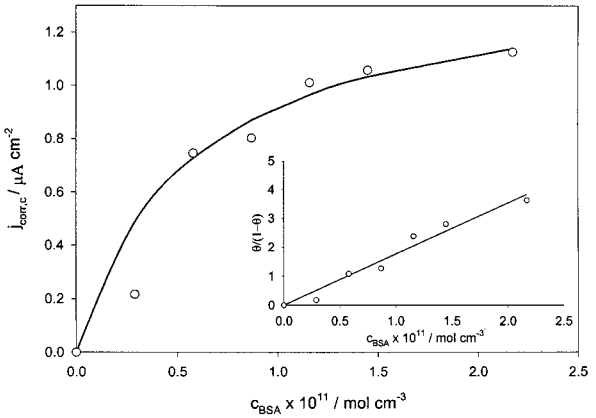

Figure 8. Adsorption isotherm of BSA adsorbed onto the stainless steel electrode in 0.05 M phosphate buffer solution pH 7.0 at 299 K. Symbols are measured values, and solid line is a curve generated from the data using the Langmuir equation for adsorption. Inset: Langmuir isotherm presented in a form of the degree of surface coverage.

surface concentration of BSA, $j_{corr,c} \propto \Gamma$. The dependence of $c/j_{corr,c}$ versus BSA concentration $c_{(BSA)}$ (eq 10) was found to be linear, with a correlation coefficient $r^2 = 0.9839$. A value $j_{corr,c(max)}$ (which is proportional to Γ_{max}) was calculated from the slope of the line to be 1.456 μA cm^{-2}. The intercept yielded $B_{ads} = 1.78 \times 10^{11}$ cm^3 mol^{-1}. By use of these values, the isotherm for the adsorption of BSA onto the stainless steel surface at 299 K was plotted according to eq 9 (Figure 8). As an inset in the same figure, the isotherm is presented in a form of the dependence of the degree of surface coverage θ on the concentration ($\theta/(1 - \theta) = B_{ads}c$, where $\theta = j_{corr,c}/j_{corr,c,(max)}$). The dependence was found to be linear, which confirmed the applicability of the Langmuir isotherm in the description of adsorption of BSA onto the stainless steel surface.

The parameter B_{ads}, which reflects the affinity of the adsorbate molecules toward adsorption sites at a constant temperature, could be presented as[54]

$$B_{ads} = \frac{1}{c_{solvent}} \exp\left(\frac{-\Delta G_{ads}}{RT}\right) \qquad (11)$$

where R (J mol^{-1} K^{-1}) is the gas constant, T (K) the temperature, ΔG (J mol^{-1}) the free energy of adsorption, and $c_{solvent}$ the molar concentration of a solvent, which is for this case the water ($c_{H_2O} = 55.5$ mol dm^{-3}). With this equation, the Gibbs free energy of adsorption of BSA onto the stainless steel surface in phosphate buffer solution at 299 K was calculated to be −57.2 kJ mol^{-1}. Such a high value indicates strong adsorption of BSA onto the stainless steel surface, i.e., chemisorption. This confirmed our previous conclusion drawn from the difference in the corrosion activation energies caused by the addition of BSA to the solution (Arrhenius plot, Figure 7). From the B_{ads} value reported in Hansen's paper,[38] the free energy of adsorption of BSA onto the stainless steel 304L powder at 298 K and pH 7.5 was calculated to be −58.5 kJ mol^{-1} which agrees very well with our present results. The value of the Gibbs free energy of adsorption of BSA onto the stainless steel surface was calculated at different temperatures, and its dependence on temperature is shown in Figure 9. From the intercept of the line, the enthalpy of adsorption was calculated to be $\Delta H_{ads} = -47.1$ kJ mol^{-1} and the slope yielded the value of entropy $\Delta S_{ads} = 33.6$ J mol^{-1} K^{-1}.

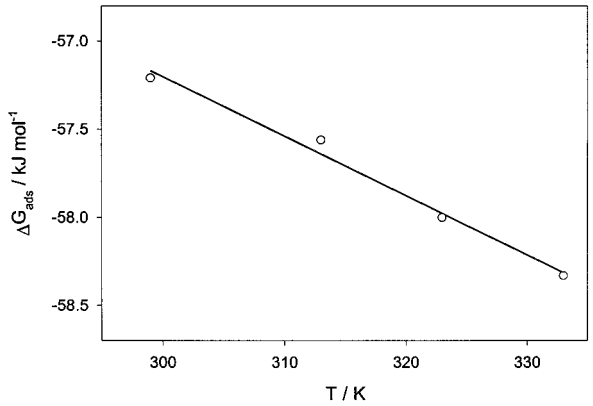

Figure 9. Dependence of the Gibbs free energy of adsorption on the temperature for BSA adsorbed onto the stainless steel electrode in 0.05 M phosphate buffer solution pH 7.0.

Conclusions

Studies of the interfacial behavior of BSA at the stainless steel electrode were conducted over the temperature range 299−343 K, using OCP, potentiodynamic LP, and EIS techniques. The electrode/electrolyte interface and corresponding surface processes were modeled by applying an EEC approach. An EEC with two time constants in parallel was found to be the most suitable for describing and modeling the investigated system.

It was shown that the adsorption of BSA onto the stainless steel surface at open circuit potential had a negative influence on the corrosion behavior of the steel; i.e., it resulted in increased metal dissolution. Adsorbed BSA molecules influenced only the anodic corrosion reaction, the rate of which was controlled by both the surface diffusion and charge transfer process. A large decrease in the corrosion activation energy, caused by the adsorption of BSA, indicated that the adsorption of protein molecules was accompanied by the transfer of charge. The adsorption process was described with a Langmuir adsorption isotherm. The calculated free energies of adsorption and enthalpy suggested a very strong adsorption of BSA molecules through chemisorption. An adsorption mechanism was proposed involving the interaction of the negatively charged carboxylate groups of the proteins as anchoring sites between the proteins and the stainless steel surface.

The present study gives some new fundamental and applicable information on the behavior of BSA at a stainless steel surface and also shows that the effect of proteins on the degradation and fouling of biomaterials and materials of construction cannot be neglected. In addition, the EIS technique was shown to be a valuable tool in studying the interfacial behavior of proteins at metal electrode surfaces.

Acknowledgment. Grateful acknowledgment is made to the Dairy Farmers of Canada and the Natural Science and Engineering Research Council of Canada for support of this research.

LA990474F

(54) Gomma, G. K.; Wahdan, M. H. *Mater. Chem. Phys.* **1994**, *39*, 142.